

## Rice phloem thioredoxin h has the capacity to mediate its own cell-to-cell transport through plasmodesmata

Yutaka Ishiwatari<sup>1,3</sup>, Toru Fujiwara<sup>1,3</sup>, K.C. McFarland<sup>3</sup>, Keisuke Nemoto<sup>2</sup>, Hiroaki Hayashi<sup>1</sup>, Mitsuo Chino<sup>1</sup>, William J. Lucas<sup>3</sup>

<sup>1</sup>Department of Applied Biological Chemistry, Graduate School of Agricultural and Life Sciences, University of Tokyo, Bunkyo-ku, Tokyo 113, Japan

<sup>2</sup>Department of Agricultural and Environmental Biology, Graduate School of Agricultural and Life Sciences, University of Tokyo, Bunkyo-ku, Tokyo 113, Japan

<sup>3</sup>Section of Plant Biology, Division of Biological Science, University of California, Davis, CA 95616, USA

Received: 6 June 1997 / Accepted 25 June 1997

**Abstract.** Rice (*Oryza sativa* L.) phloem sieve tubes contain RPP13-1, a thioredoxin h protein that moves around the plant via the translocation stream. Such phloem-mobile proteins are thought to be synthesized in the companion cells prior to being transferred, through plasmodesmata, to the enucleate sieve-tube members. In this study, in-situ hybridization experiments confirmed that expression of *RPP13-1* is restricted to companion cells within the mature phloem. To test the hypothesis that RPP13-1 enters the sieve tube, via plasmodesmata, recombinant RPP13-1 was expressed in *Escherichia coli*, extracted, purified and fluorescently labeled with fluorescein isothiocyanate (FITC) for use in microinjection experiments into tobacco (*Nicotiana tabacum* L.) mesophyll cells. The FITC-RPP13-1 moved from the injected cell into surrounding cells, whereas the *E. coli* thioredoxin, an evolutionary homolog of RPP13-1, when similarly labeled and injected, failed to move in this same experimental system. In addition, co-injection of RPP13-1 and FITC-dextran established that RPP13-1 can induce an increase in plasmodesmal size exclusion limit to a value greater than 9.4 but less than 20 kDa. Nine mutant forms of RPP13-1 were constructed and tested for their capacity to move from cell to cell; two such mutants were found to be incapable of movement. Crystal-structure prediction studies were performed on wild-type and mutant RPP13-1 to identify the location of structural motifs required for protein trafficking through plasmodesmata. These studies are discussed with respect to plasmodesmal-mediated transport of macromolecules within the companion cell-sieve tube complex.

**Key words:** Companion cell-sieve tube system – *Nicotiana* – *Oryza* (phloem thioredoxin) – Phloem function – Plasmodesmata (protein trafficking) – Thioredoxin (mutants)

### Introduction

In higher plants, the phloem functions as a special conduit for the long-distance transport of carbohydrates, amino acids, and other nutrients from source to sink tissues. In addition, macromolecules such as proteins and nucleic acids have been detected in the phloem sap and a range of enzymatic activities have been shown to be associated with phloem exudate collected from a number of plant species (Eschrich and Heyser 1975; see also Komor et al. 1996). These observations indicated that the proteins present within the phloem sap may be involved in the catalysis of biochemical reactions required for sieve-tube function. However, this hypothesis has been challenged on the basis that the collected phloem exudate was contaminated by proteins released from surrounding cells that were damaged in the process of collecting the exudate.

Pure phloem sap can be collected from plants using either an insect laser (Kawabe et al. 1980) or microcautery (Fisher et al. 1992) technique. The existence of many proteins (over 100) within wheat and rice phloem sap, collected from severed insect stylets, was established using two-dimensional polyacrylamide gel electrophoresis (Fisher et al. 1992; Nakamura et al. 1993). A partial amino acid sequence of an abundant protein present as a rice phloem protein, RPP13-1, enabled the identification of this specific RPP as a member of the thioredoxin h (TRX h) gene family (Ishiwatari et al. 1995). Thioredoxins are ubiquitous low-molecular-mass proteins that function to reduce disulfide bonds on target proteins (Holmgren 1985). In higher plants, two forms of TRX have been characterized (Johnson et al. 1987); the chloroplastic TRXs (type m and f) are involved in

Abbreviations: FITC = fluorescein isothiocyanate; LYCH = Lucifer yellow CH; RPP = rice phloem protein; SEL = size exclusion limit; TMV-MP = tobacco mosaic virus movement protein; TRX = thioredoxin

Correspondence to: W.J. Lucas; E-mail: wjlucas@ucdavis.edu;  
Fax: 1(916) 752 5410

activating a number of chloroplast enzymes, and the cytoplasmic TRXs (type h), which are reduced by an NADPH-dependent TRX reductase, similarly appear to be involved in the activation of a number of cytosolic enzymes. Based on the known functions of TRX h within the cytoplasm of plant cells, Ishiwatari et al. (1995) proposed that RPP13-1 is involved in disulfide reduction within the sieve tubes. For example, RPP13-1 may be essential for the repair of oxidatively damaged proteins in sieve tubes, as TRX has been shown to regenerate proteins that have been inactivated by oxidative stress *in-vitro* (Pigiet and Schuster 1986) or *in-vivo* (Fernando et al. 1992).

The molecular identification of RPP13-1, obtained from pure rice phloem sap, as a TRX h, provided strong support for the above-stated hypothesis that specific proteins, present within the phloem sap of higher plants, mediate biochemical events required for phloem function. It is well known that mature sieve elements of higher plants lack nuclei, and ribosomes are either absent or present in extremely low numbers. As the enucleate sieve tubes remain functional from days to months, it is logical to assume that routine maintenance functions must be performed by the neighboring companion cells. Ultrastructural studies have established that individual sieve-tube members are connected to companion cells by specialized plasmodesmata (Lucas et al. 1993). Thus, proteins like RPP13-1 (TRX h) (and presumably metabolic substrates like ATP, NADPH, etc.) required for sieve-tube repair/function could be synthesized in the companion cell and then transported, through the connecting plasmodesmata, to the lumen of the functional sieve tube (Raven 1991). Indirect experimental support for this hypothesis has been provided by Fisher et al. (1992) who demonstrated that, in wheat plants, [<sup>35</sup>S]methionine-labeled proteins located within the functional sieve tubes underwent rapid turnover, with the label being confined primarily to the companion cell-sieve tube complex.

Direct evidence that higher-plant plasmodesmata have the capacity to mediate cell-to-cell trafficking of proteins has recently been provided by studies performed on plant viral movement proteins and endogenous transcription factors (Lucas et al. 1995; Mezitt and Lucas 1996, and references therein). In these studies, protein trafficking through plasmodesmata was found to correlate with an induced increase in molecular size exclusion limit (SEL) from a control value of approx. 1 kDa to a value above 10 kDa but less than 40 kDa. Microinjection experiments have also been used to establish that the SEL of the plasmodesmata connecting the companion cell-sieve tube complex in the stem of *Vicia faba* is above the 1-kDa value detected for normal plant cells, being greater than 10 kDa (Kempers et al. 1996). This finding is consistent with the observation that the plasmodesmal SEL undergoes an increase during cell-to-cell trafficking of macromolecules (proteins and protein-nucleic acid complexes; Gilbertson and Lucas 1996). Finally, recent studies on source leaves of potato, tobacco and tomato have provided strong evidence that at least one mRNA can enter the

plasmodesmata that interconnect the companion cell-sieve tube complex (Kühn et al. 1997). Presumably the trafficking of this mRNA, encoding the 100-kDa sucrose transporter which is an integral membrane protein located within the sieve-tube plasma membrane, occurs as a ribonucleoprotein complex.

In the present study, RPP13-1 was employed as a representative member of the rice phloem proteins to determine whether it has the capacity to mediate its own cell-to-cell movement. Consistent with its role in phloem function, *in-situ* experiments revealed that RPP13-1 mRNA was expressed only in the companion cells of the rice phloem. Although technical difficulties prevented us from performing microinjection experiments on rice phloem cells, we were able to obtain direct proof that RPP13-1 has the capacity to increase plasmodesmal SEL and mediate its own trafficking through tobacco mesophyll plasmodesmata. Mutational analysis performed on RPP13-1 and parallel microinjection studies carried out with bacterial TRX confirmed that structural motifs on the RPP13-1 are critical for this cell-to-cell movement. These findings are discussed in terms of the evolution and function of macromolecular trafficking between the companion cells and the functional sieve-tube system of higher plants.

## Materials and methods

**Plant material.** Rice plants (*Oryza sativa* L. cv. Kantou) were grown under hydroponic culture conditions at controlled temperature as described by Nakamura et al. (1993). Tobacco plants (*Nicotiana tabacum* L. cv. Turkish Samsun NN) were grown in a greenhouse under natural sunlight (average midday irradiance of 1000  $\mu\text{mol} \cdot \text{m}^{-2} \cdot \text{s}^{-1}$ ) and day/night temperatures of 26 °C/18 °C, respectively. Plants were watered with half-strength Hoagland's solution (Hoagland and Arnold 1938) twice daily. Five-week-old plants were transferred to a controlled-environment chamber for preconditioning (7 d) prior to use in microinjection experiments.

***In-situ* hybridization procedures.** Digoxigenin-labeled antisense and sense RNA probes were synthesized using T3 RNA polymerase (Ambion, Austin, Tex., USA) and partially hydrolyzed with sodium carbonate. The basal region (5 mm length) of three-week-old rice plants was excised and fixed in 4% (w/v) paraformaldehyde and 0.25% (w/v) glutaraldehyde in 50 mM sodium phosphate buffer (pH 7.2). Tissue was then dehydrated and embedded in paraffin wax as described by Kouchi and Hata (1993). Thick sections (10  $\mu\text{m}$ ) were cut using a microtome and then transferred to glass slides that had been treated with 3-aminopropyltriethoxysilane. *In-situ* hybridizations with antisense and sense probes were carried out following the method of Kouchi and Hata (1993).

**Production of wild-type and mutant RPP13-1 in *E. coli*.** A fragment containing the open reading frame encoding RPP13-1 was excised from cRPP13-1 (described in Ishiwatari et al. 1995) with *EaeI* and *EcoRI*. The pMAL-c2 vector (New England Biolabs, Beverly, Mass., USA) was digested with *EcoRI*. The fragment and the pMAL-c2 vector were ligated after being blunt-ended with Klenow enzyme. This construct was verified, via sequence analysis, prior to being introduced into *E. coli* TB1 strain. A fusion protein, consisting of maltose-binding protein and the RPP13-1 with additional amino acids at the N-terminus, was produced in *E. coli*.

For RPP13-1 mutant proteins, the 5' untranslated sequence of the cDNA encoding RPP13-1 was first mutated by site-directed mutagenesis using an oligonucleotide primer to generate a new

*Bst*XI site. Further mutations were engineered into this cDNA by using nine primers to generate both alanine scanning and deletion mutants. Wild-type RPP13-1 has seven clusters of charged amino acid residues and these were each, separately, changed to alanines. Two deletion mutations were engineered; in the first, five amino acid residues were deleted from the N-terminus, while in the second, seven amino acid residues were deleted from the C-terminus. The seven alanine scanning mutants and the C-terminal deletion mutant were digested with *Bst*XI and then blunt-ended by T4 DNA Polymerase (Takara Shuzo Co., Otsu, Japan); subsequent digestion with *Eco*RI produced the other ends. The fragment containing the N-terminal deletion mutant was digested at the *Sma*I site, which was introduced within the open reading frame, to generate one end, while the other end was made by digestion with *Eco*RI. The fragments so produced were ligated to the linearized vector pMALc-2h, that was then linearized by digestion with *Xmn*I and *Eco*RI. The recombinant plasmids were introduced into *E. coli* XL1-Blue strain.

The fusion proteins were expressed and purified following the manufacturer's instructions (New England Biolabs). Fusion proteins were then cleaved with factor Xa protease (New England Biolabs) to remove all additional residues from wild-type and mutant forms of RPP13-1, which were then separated from the excised maltose-binding protein and concentrated by filtration with Centrprep concentrators (Amicon, Beverly, Mass., USA).

**Microinjection protocol.** A tobacco leaf was fixed, adaxial side up, onto a glass plate that was attached to the stage of a Leitz Orthoplan epi-illumination microscope. A small portion of the lower epidermis was peeled off to provide access to mesophyll cells. Distilled water, or 0.1 M mannitol, was immediately applied to the exposed region of the leaf. Details regarding the instrumentation and procedures for pressure-mediated microinjection were as previously described (Ding et al. 1992). Purified RPP13-1 and the engineered RPP13-1 mutant forms were labeled with fluorescein isothiocyanate (FITC) using the method of Noueir et al. (1994). Before being employed in microinjection experiments, FITC-labeled protein solutions were subjected to SDS-PAGE to ensure that they were free from unincorporated molecules of FITC. To monitor mesophyll plasmodesmal function and SELs, Lucifer yellow CH (LYCH; 457 Da), 9.4-kDa and 20-kDa fluorescein-conjugated dextrans (FITC-dextran), all at 1 mM, were prepared in 5 mM KHCO<sub>3</sub>, filtered through a 0.1- $\mu$ m-pore polyvinylidenedifluoride membrane filter (Ultrafree C3 VV; Millipore, Bedford, Mass., USA), and stored at 4 °C until used in injection experiments. Protein concentrations (wild-type and mutants) used in microinjection experiments were between 1.0 and 3.0 mg · ml<sup>-1</sup>.

Tobacco mosaic virus movement protein (TMV-MP) was prepared and FITC-labeled using the strains and protocols described in Nguyen et al. (1996).

**Wild-type and mutant RPP13-1 structure predictions.** The BLASTP program (version 1.3.11) of Altschul et al. (1990) was applied to the ExpDB-modified PDB database of protein sequences to identify known crystal structures having the highest level of sequence identity to RPP13-1. Three such crystal structures representing human (1ERT), *Chlamydomonas* (1TOF) and *E. coli* (1XOA) TRXs were selected and employed, separately and jointly, as a foundation for the construction of homologous RPP13-1 crystals using the Swiss Model server which makes use of ProMod (PROtein MODELing tool, Peitsch 1996). Wild-type and mutated sequences of *RPP13-1* were used in these structure-prediction studies.

## Results

**In-situ localization of rice RPP13-1 mRNA.** To confirm that the mRNA encoding RPP13-1 is expressed within the companion cells of the rice phloem, in-situ hybrid-

ization experiments were performed using digoxigenin-labeled antisense RPP13-1 h RNA as a probe. Ishiwatari et al. (1995) collected pure rice phloem sap containing RPP13-1 from severed stylets of brown planthoppers that were feeding on the leaf sheath and stem of young rice plants. In-situ studies performed on equivalent leaf sheath tissue revealed that *RPP13-1* mRNA accumulation occurred only in the phloem tissue, and specifically in companion cells (Fig. 1A,E). Similar experiments performed on rice stem tissues indicated that expression of the *RPP13-1* mRNA was also restricted to the companion cells within the mature phloem (Fig. 1C,F). Rice tissues incubated with *RPP13-1* sense RNA probe established the specificity of these results (Fig. 1B,D). These data are consistent with the hypothesis that the RPP13-1 is first synthesized in the companion cell before being transported into neighboring sieve elements, via plasmodesmata.

*RPP13-1 has the capacity to traffic from cell to cell.* The RPP13-1 expressed in *E. coli* was extracted, purified and fluorescently labeled with fluorescein isothiocyanate (FITC-RPP13-1). It was our intention to pressure-inject FITC-RPP13-1 directly into the companion cells located within the phloem of the rice leaf sheath. Earlier microinjection studies had established the feasibility of this approach, but, with one exception, these experiments were conducted on special phloem tissues located within stems (see Kempers et al. 1996 and references therein). Preliminary experiments revealed that it was almost impossible to gain access to the leaf sheath tissues, as it was extremely difficult to remove the lower epidermis of this monocot without damaging the underlying tissues. Furthermore, the technical difficulties associated with performing injections into exposed vascular tissues clearly indicated the need to seek an alternative experimental tissue in which to perform these microinjection studies. As Lucas et al. (1995) had established that KNOTTED1, a homeobox domain protein that functions in the meristem of maize, has the capacity to traffic through plasmodesmata located in other maize tissues (mesophyll), as well as plasmodesmata in heterologous tissues (tobacco mesophyll), a similar heterologous system was employed for the present studies.

Introduction of FITC-RPP13-1 into tobacco mesophyll cells resulted in the spread of fluorescence from the injected cell into the neighboring cells within less than one min. In Fig. 2A we present a typical example from such a microinjection experiment in which the fluorescence associated with FITC-RPP13-1 can be seen within the surrounding mesophyll cells. We next injected an evolutionary homolog of RPP13-1, namely TRX from *E. coli*. In all cases, the FITC-labeled TRX from *E. coli* failed to move out of the injected cell (Fig. 2B; Table 1). Given that both proteins were prepared using identical procedures, the inability of *E. coli* FITC-TRX to move from cell to cell confirms that the observed spread of fluorescence in FITC-RPP13-1 injections reflects bona fide movement-dependent properties associated with this rice phloem protein. It is also important to stress that,

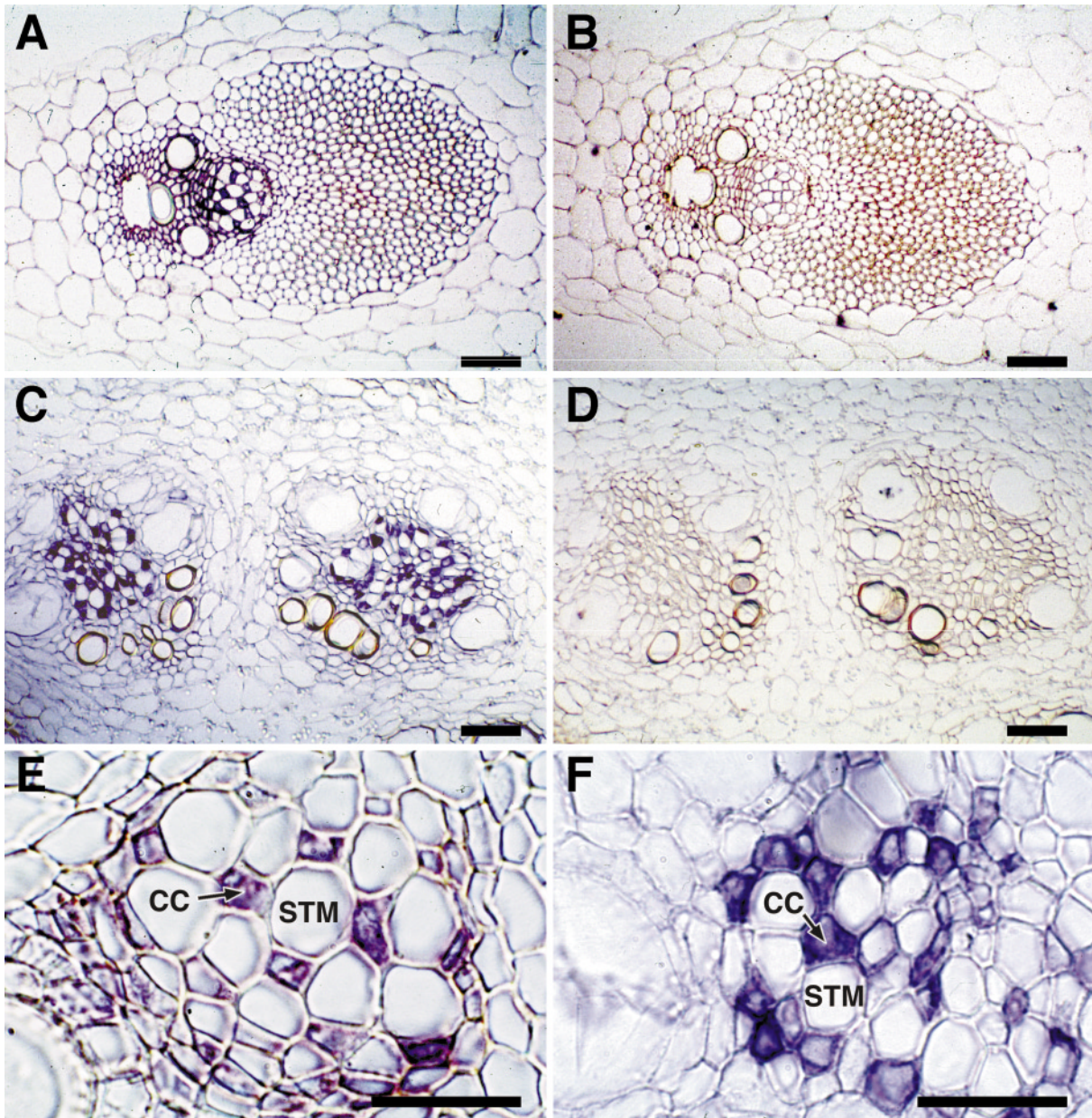


**Fig. 1A–F.** Presence of mRNA encoding *RPP13-1* in companion cells of mature phloem within the leaf sheath and stem tissues of rice (*Oryza sativa* L.). In-situ hybridizations performed on rice leaf sheath (A, B, E) and stem (C, D, F) cross-sections. Tissues were hybridized with digoxigenin-labeled antisense (A, C, E, F) or sense (B, D) riboprobes generated from *RPP13-1* cDNA. Note the presence of strong hybridization signal associated with the companion cells (CC) located in the leaf sheath (A, E) and stem (C, F) phloem and the absence of label in the sense controls (B, D). STM, sieve tube member. Bars = 20  $\mu$ m

prior to injecting either FITC-RPP13-1 or *E. coli* FITC-TRX, the injection solutions were first analyzed to establish the purity of the protein and to confirm that these preparations were indeed free of unincorporated FITC molecules (Fig. 3).

The frequency with which microinjected FITC-RPP13-1 moved in this heterologous tissue (65%;

Table 1) was lower than that observed for FITC-KNOTTED1 injected into similar tobacco mesophyll cells (88%, Lucas et al. 1995). Control experiments performed with the small, membrane-impermeable fluorescent probe, LYCH, indicated that these mesophyll plasmodesmata were not affected by tissue preparation, as cell-to-cell movement of dye occurred in almost every case (Tables 1, 2). Experiments performed with FITC-labeled movement protein of tobacco mosaic virus (TMV-MP) provided an internal standard for the expected efficiency of cell-to-cell movement in this plant tissue. In these experiments the TMV-MP moved in 90% of the injection experiments (Table 1).

In the process of cell-to-cell movement, all viral movement proteins tested thus far (in mesophyll microinjection experiments), as well as KNOTTED1, induce

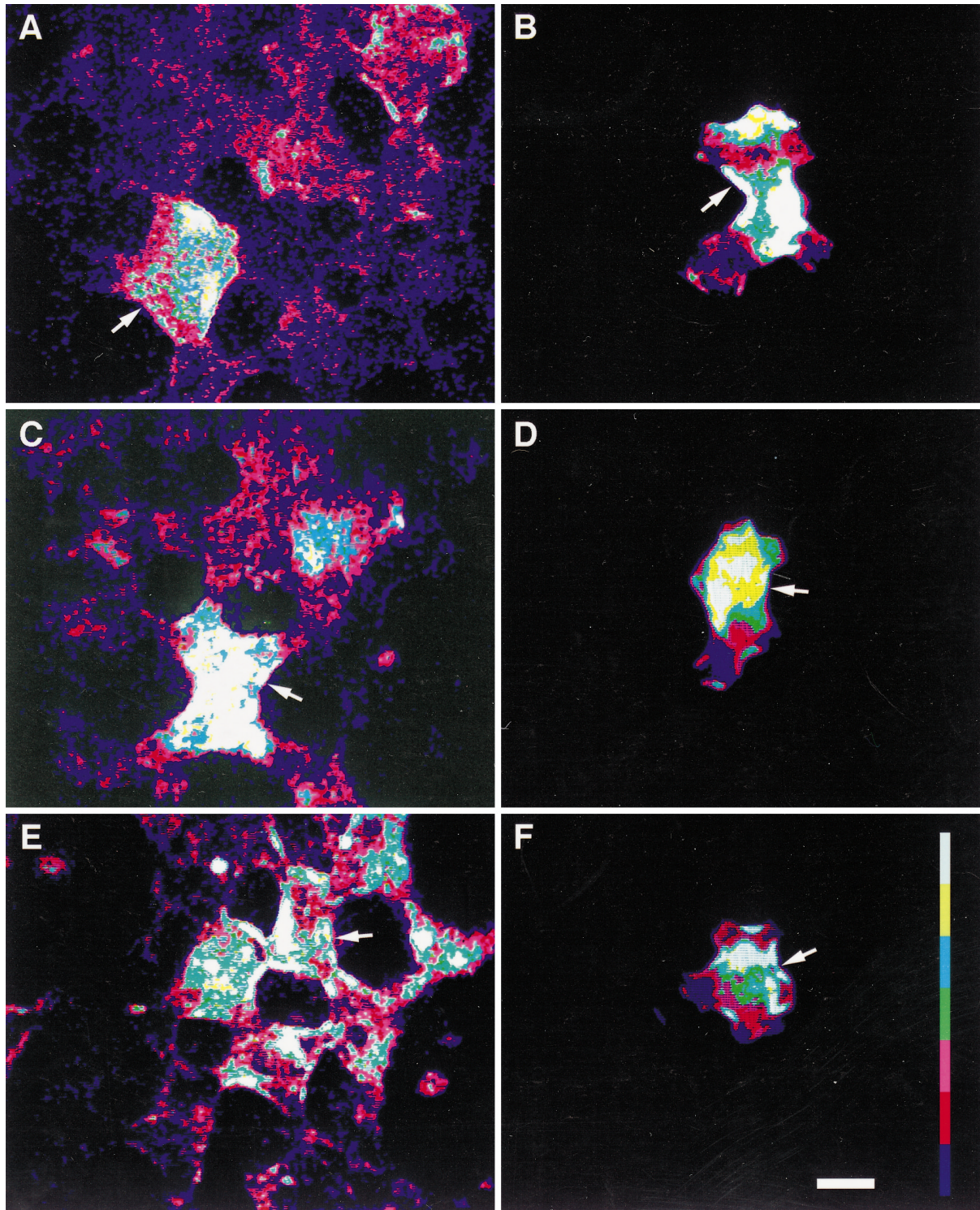


**Fig. 2A–F.** Cell-to-cell movement of FITC-labeled RPP13-1 and its effect on plasmodesmal SEL in tobacco mesophyll cells. Wild-type and mutant (MT1, MT9) forms of RPP13-1 were expressed in *E. coli* and extracted, purified, proteins were labeled with FITC prior to being used in microinjection studies. Shortly after being pressure-injected into a mesophyll cell, FITC-RPP13-1 moved into surrounding cells as indicated by false-color images obtained with an Hamamatsu model C1966-20 analytical system (background was black, and white represented the highest intensity employed; see color bar in F.) All images presented were collected 5 min after microinjection into a target cell (identified by an *arrow*). **A** Microinjection of FITC-RPP13-1 into tobacco mesophyll cell. **B** *Escherichia coli* FITC-TRX failed to move from the target cell. **C, D** Co-injection of unlabeled RPP13-1 and 9.4- and 20-kDa FITC-dextran, respectively, into a tobacco mesophyll cell. **E** Cell-to-cell movement of FITC-RPP13-1 MT9. **F** Containment of FITC-RPP13-1 MT1 within mesophyll cell. Bar = 50  $\mu$ m (common for A–F)

**Table 1.** Rice phloem protein 13-1 interacts with plasmodesmata to increase the SEL of tobacco mesophyll cells and potentiates its own cell-to-cell transport. RPP13-1 was overexpressed in *E. coli* (as a fusion to a maltose-binding protein), extracted from inclusion bodies, purified and conjugated to fluorescein isothiocyanate (FITC-RPP13-1) as described in *Materials and methods* prior to use in microinjection experiments performed on tobacco mesophyll cells. Fluorescent images were detected and recorded using a Hamamatsu model C1966-20 analytical system

Injected material	Microinjections	
	Total (N)	Movement <sup>a</sup> (N [%])
LYCH <sup>b</sup>	20	19 (95%)
9.4-kDa FITC-dextran	20	1 (5%)
FITC-RPP13-1	20	13 (65%)
<i>E. coli</i> FITC-TRX	15	0 (0%)
RPP13-1 + 9.4-kDa FITC-dextran	24	13 (54%)
RPP13-1 + 20-kDa FITC-dextran	20	2 (10%)
TMV FITC-MP	10	9 (90%)

<sup>a</sup>Number of injections and percent of total injections in which the fluorescently labeled probe moved from the injected cell into the surrounding mesophyll tissue

<sup>b</sup>At the commencement of each experiment, the status of plasmodesmata within the tobacco mesophyll was tested with LYCH and 9.4-kDa FITC-dextran

an increase in plasmodesmal SEL (Lucas and Gilbertson 1994; Mezitt and Lucas 1996). As expected, when 9.4-kDa FITC-dextran was microinjected on its own into mesophyll cells, fluorescence remained within the injected cell (Table 1). However, co-injection of this 9.4-kDa FITC-dextran with unlabeled RPP13-1 resulted in the movement of fluorescence from the injected cell into the surrounding mesophyll (Fig. 2C). The increase in plasmodesmal SEL induced by RPP13-1 was found to be greater than 10 kDa but less than 20 kDa, as co-injection of RPP13-1 and 20-kDa FITC-dextran did

**Table 2.** Ability of RPP13-1 mutants to traffic cell to cell through tobacco mesophyll tissue

Injected material <sup>a</sup>	Microinjections		Extent of movement <sup>c</sup>
	Total (N)	Movement <sup>b</sup> (N [%])	
LYCH	59	59 (100%)	+++
9.4-kDa FITC-dextran	54	0 (0%)	-
FITC-RPP13-1	66	41 (62%)	+→++++
FITC-RPP13-1 MT1 <sup>d</sup>	20	0 (0%)	-
FITC-RPP13-1 MT2	21	7 (33%)	+→++++
FITC-RPP13-1 MT3	19	8 (42%)	+→++++
FITC-RPP13-1 MT4	20	8 (40%)	+→++++
FITC-RPP13-1 MT5	22	8 (36%)	+→++++
FITC-RPP13-1 MT6	20	10 (50%)	+→++++
FITC-RPP13-1 MT7	20	6 (30%)	+→++++
FITC-RPP13-1 MT8	20	2 (10%)	+
FITC-RPP13-1 MT9	20	8 (40%)	+→++++

<sup>a</sup>Experimental details as in Table 1

<sup>b</sup>Number of injections and percent of total injections in which the fluorescently labeled probe moved from the injected cell into the surrounding mesophyll tissue

<sup>c</sup>Extent of cell-to-cell movement for the various probes was as follows: - no movement out of the injected mesophyll cell; + movement restricted to neighboring cells; +++ extensive movement throughout the field of view (approx. 30 cells)

<sup>d</sup>Details on the amino acid changes engineered for each RPP13-1 mutant are given in Fig. 4

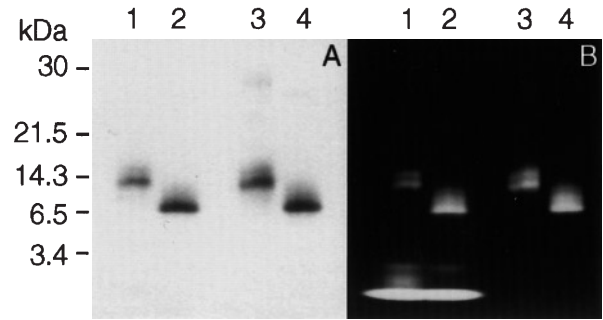


**Fig. 3A,B.** Analysis of FITC-labeled RPP13-1 and *E. coli* TRX by SDS-PAGE. Both FITC-RPP13-1 and bacterial FITC-TRX were prepared as described in *Materials and methods* prior to being analyzed on a 15% SDS-polyacrylamide gel. Equal quantities (3  $\mu$ g) of RPP13-1 and *E. coli* TRX were loaded onto the gels. Protein molecular-weight markers are indicated to the left. **A** Gel image visualized by Coomassie Blue staining. **B** Gel image visualized using a UV-transilluminator. Lanes are as follows: 1, undialyzed FITC-RPP13-1; 2, undialyzed *E. coli* FITC-TRX; 3, dialyzed FITC-RPP13-1; 4, dialyzed *E. coli* FITC-TRX

not result in the spread of fluorescence from the injected mesophyll cell (Fig. 2D, Table 1).

*Analysis of RPP13-1 mutant proteins.* To analyze the structural aspects of the RPP13-1 required for plasmodesmal trafficking, a number of mutations were engineered in this rice phloem protein. In comparison with *E. coli* TRX, RPP13-1 contains additional amino acids at both its N- and C-termini (Fig. 4). To test whether the additional amino acid residues on RPP13-1 are involved in forming a structural motif that permits cell-to-cell movement of this protein, RPP13-1 mutants were engineered in which five and seven amino acid residues were deleted from the N- and C-terminus, respectively. In addition, using site-directed mutagenesis, seven alanine scanning mutants were also engineered for

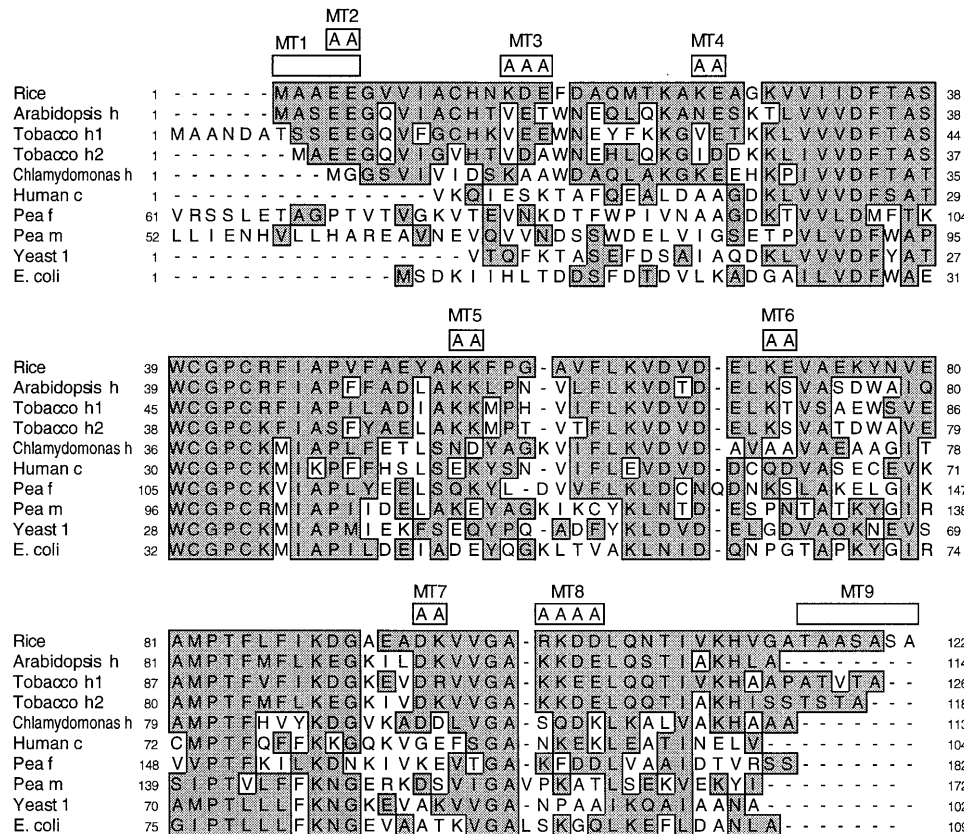


**Fig. 4.** Comparison of the predicted amino acid sequence for the protein encoded by cRPP13-1 (RPP13-1) and other TRXs. Sequences were aligned using the pileup program, Wisconsin package version 9.0, Genetics Computer Group (Madison Wis., USA). *Arabidopsis h* (Rivera-Madrid et al. 1995), tobacco h1 (Marty and Meyer 1991), tobacco h2 (Brugidou et al. 1993), *Chlamydomonas h* (Stein et al. 1995), human c (Qin et al. 1994), pea f (Lepiniec et al. 1992) and m (López-Jaramillo et al. 1994) – note sequences for f and m were truncated to conserve space, yeast 1 (Gan 1991), *E. coli* (Holmgren 1985; Katti et al. 1990; Jeng et al. 1994). Shaded boxes highlight those residues that have similarity or identity with RPP13-1, based on the PAM250 Dayhoff matrix. RPP13-1 deletion and alanine scanning mutants generated to identify protein domains required for RPP13-1-plasmodesmal interaction are indicated by horizontal boxes, with the assigned number of each mutant indicated above the site. Deletion mutants were generated by the removal of the residues located below the boxed regions

experimental testing. The sites of the engineered mutations within the *RPP13-1* gene are indicated in Fig. 4. Microinjection experiments performed using the RPP13-1 mutant MT1, in which the N-terminal 5 amino acids had been deleted, indicated that this protein was incapable of moving from cell to cell (Fig. 2F, Table 2). Interestingly, the C-terminal seven-amino-acid deletion form of the RPP13-1 (MT9) was still capable of moving through mesophyll plasmodesmata (Fig. 2E), albeit at a reduced level of efficiency (Table 2).

Microinjection experiments performed on the seven RPP13-1 alanine scanning mutants (MT2–MT8) revealed that all but one (MT8) retained the capacity to interact with tobacco mesophyll plasmodesmata to mediate their own cell-to-cell transport (Table 2). The only detectable difference between wild-type protein and these mutant forms of the RPP13-1 was in the efficiency of movement out of the injected cell; for the mutant proteins, this ranged from 30 to 50% in comparison with 62% for wild-type RPP13-1. As indicated by the data presented in Table 2, when they did move from the injected cell into the surrounding tissue, the extent of movement of alanine scanning mutants MT2–MT7 was similar to that observed for wild-type RPP13-1.

*Influence of mutations on the predicted crystal structure of RPP13-1.* Mutations engineered within RPP13-1 could influence its capacity to move from cell to cell by deleting/altering residues essential for binding to cellular components involved in delivery and/or transport through plasmodesmata. Alternatively, such mutations

could significantly alter the tertiary structure of RPP13-1 thereby rendering it inactive. As RPP13-1 MT1 and MT8 were unable to move out of the injected cell, we used the BLASTP and ProMod programs to explore the likely influence of these changes on the overall predicted structure of RPP13-1. For these studies, three TRXs (human, *Chlamydomonas* and *E. coli*) having the highest level of sequence identity to RPP13-1 (see Fig. 4) and for which known crystal structures are available were used as a foundation for the construction of homologous RPP13-1 crystals.

Based on our structural prediction analyses, deletion of the N-terminal five residues from RPP13-1 (MT1) would have had little influence over the backbone structure of the protein (Fig. 5A). Note that the predicted locations of the active-site cysteines in the wild-type and the MT1 form of RPP13-1 were identical. Furthermore, biochemical studies performed with wild-type and mutant forms of RPP13-1 confirmed their dithiol reductase activity, in that they were able to catalyze the reduction of insulin disulfide (data not shown). Thus, the important structural difference between these two proteins appears to be that the N-terminus of MT1 does not project into the interior of the protein and, probably more importantly, the two charged residues (Glu<sub>4</sub>-Glu<sub>5</sub>) that are predicted to project out from the surface of the wild-type protein (see also Fig. 5C) are absent in the RPP13-1 MT1 mutant protein. Note also that the MT1 N-terminal residues (Gly<sub>1</sub>-Val<sub>2</sub>) do not project out from the surface of the protein and, in this configuration, the protein was

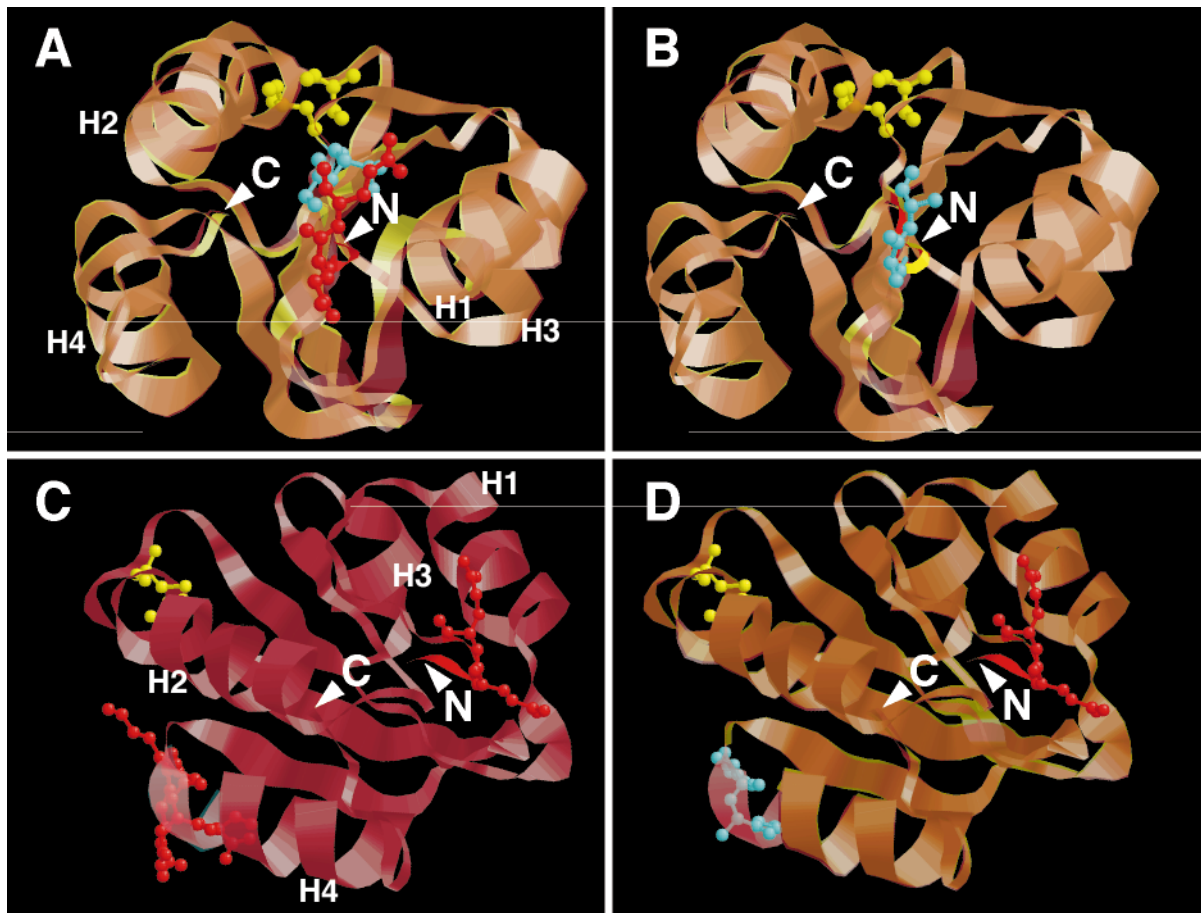


**Fig. 5A–D.** Predicted ribbon structures for wild-type (**C**, red) and mutant (**A**, **B**, **D**, yellow) forms of RPP13-1. Alanine replacements are shown in light blue, the active-site cysteines are shown in yellow ball and stick. Mutant structures are shown overlaying the wild-type structure in **A**, **B** and **D** and coincident residues appear copper in color. **A** Residues Glu<sub>4</sub>-Glu<sub>5</sub> of wild-type RPP13-1 depicted in red ball and stick, whereas RPP13-1 MT1 N-terminal residues 1–2 (i.e., wild-type residues Gly<sub>6</sub>-Val<sub>7</sub>) are depicted in light-blue ball and stick. **B** Residues Ala<sub>4</sub>-Ala<sub>5</sub> of RPP13-1 MT2 are depicted in light-blue ball and stick. **C** A rotated view of RPP13-1 showing ribbon structure with residues Glu<sub>4</sub>-Glu<sub>5</sub> and Arg<sub>101</sub>-Lys<sub>102</sub>-Asp<sub>103</sub>-Asp<sub>104</sub> depicted in red ball and stick. **D** Wild-type residues Glu<sub>4</sub>-Glu<sub>5</sub> and MT8 residues Ala<sub>101</sub>-Ala<sub>102</sub>-Ala<sub>103</sub>-Ala<sub>104</sub> depicted in red and light-blue ball and stick, respectively. Predicted position of N- and C-termini indicated by white darts and location of alpha helices by H<sub>1</sub> to H<sub>4</sub>. (See text for details relating to methods and programs used to generate these predicted structures.)

unable to mediate its own cell-to-cell transport through plasmodesmata. Replacement of Glu<sub>4</sub>-Glu<sub>5</sub> with Ala<sub>4</sub>-Ala<sub>5</sub> also appeared to cause little modification to the backbone structure of RPP13-1 (Fig. 5B; MT2). The presence of these alanine residues on the surface of the protein appeared to potentiate a limited interaction between RPP13-1 MT2 and plasmodesmata (Table 2). These analyses support the hypothesis that the structural motif located in the N-terminus (presumably centred on residues Glu<sub>4</sub>-Glu<sub>5</sub>) of the wild-type RPP13-1 is necessary, but not sufficient, for transport through mesophyll plasmodesmata.

Microinjection experiments established that the MT8 form of RPP13-1 was also dysfunctional in terms of mediating its own cell-to-cell transport (Table 2). Here the substitution of the surface charge cluster (Arg<sub>101</sub>-Lys<sub>102</sub>-Asp<sub>103</sub>-Asp<sub>104</sub>) with Ala<sub>101</sub>-Ala<sub>102</sub>-Ala<sub>103</sub>-Ala<sub>104</sub> similarly had little or no influence on the predicted tertiary structure of RPP13-1 (Fig. 5D). Thus, it would appear that two clusters of charged residues, Glu<sub>4</sub>-Glu<sub>5</sub> and Arg<sub>101</sub>-Lys<sub>102</sub>-Asp<sub>103</sub>-Asp<sub>104</sub>, predicted to project from the surface of RPP13-1, function in some way to mediate in the binding and/or transport of this protein through mesophyll and, presumably, companion cell-sieve tube complex plasmodesmata.

## Discussion

In higher plants, enucleate sieve-tube members establish the conduit for long-distance translocation of photosynthate, amino acids and mineral nutrients. Although the longevity of an individual sieve tube can vary, they appear to remain functional for many weeks. In the absence of nuclei within individual sieve-tube members, the responsibility for cellular maintenance may have been transferred to neighboring companion cells (Raven 1991). If this were the case, expression of specific genes within individual companion cells should give rise to the presence of the encoded protein within the sieve tube



(member), via protein transport through the interconnecting plasmodesmata.

The results of the present study provide strong support for this concept. First, we show that the *RPP13-1* mRNA, encoding a rice TRX h, is localized to companion cells of the mature phloem located within the rice leaf sheath and stem. Second, phloem sap extracted from this same region of the plant was shown previously to contain a number of proteins, including RPP13-1 (Nakamura et al. 1993; Ishiwatari et al. 1995). Third, although we could not conduct experiments on rice companion cells, our microinjection experiments did establish that RPP13-1 has the capacity to interact with tobacco mesophyll plasmodesmata to induce an increase in SEL and mediate its own transport from cell to cell. The inability of *E. coli* TRX, an evolutionary homolog, to display these plasmodesmal-specific properties, as well as the loss of function associated with two mutant forms of RPP13-1, is consistent with the hypothesis that unique structural motifs are required for the observed protein trafficking through tobacco mesophyll plasmodesmata. Clearly, these studies can only provide *indirect* support for the hypothesis that RPP13-1 has the capacity to traffic, via plasmodesmata, from the rice companion cell into the sieve-tube member. At this point we should also stress that the plasmodesmata of companion cells and sieve-tube members may exhibit special characteristics that are absent from tobacco mesophyll plasmodesmata.

Studies performed on the phloem of wheat (Fisher et al. 1992), rice (Nakamura et al. 1993), cucurbits (Bostwick et al. 1992) and *Ricinus communis* (Sakuth et al. 1993; Schobert et al. 1995) now provide irrefutable evidence that the translocation stream (sieve-tube sap) contains a large number of proteins. Whether each individual protein has the capacity to interact with companion cell-sieve tube complex plasmodesmata, to gain entry into the phloem translocation stream, has yet to be determined. As RPP13-1 was able to interact with and traffic through tobacco mesophyll plasmodesmata, it is possible that such supracellular transport is controlled at several levels. Proteins that have the capacity to traffic through plasmodesmata (proteins within the phloem sap, specific plant transcription factors and viral movement proteins) may contain a common motif essential for actual transport through the plasmodesmal micro-channels. Additional cell-specific factors appear to be involved in regulating (inhibiting or facilitating) protein trafficking through specific plasmodesmata (Mezitt and Lucas 1996).

Rice companion-cell-specific factors are unlikely to be present within tobacco mesophyll cells, which could account for our finding that the RPP13-1 was not as efficient as the tobacco mosaic virus movement protein (TMV-MP) in terms of its transport through tobacco mesophyll plasmodesmata. Possible insight into the nature of these regulatory elements can be gained from a recent study in which the genes encoding two TRX h-like proteins were isolated. The yeast two-hybrid system was employed to show that these TRX-like proteins specifically interacted with the protein kinase domain of the *S*-locus receptor kinase (Bower et al. 1996). Thus, it

is possible that a motif on the RPP13-1 might interact with a specific protein kinase(s) that regulates, for example, the SEL of plasmodesmata. This regulatory aspect of companion cell-sieve tube complex plasmodesmal function will be addressed in future studies.

The [<sup>35</sup>S]-methionine-labeling studies performed on wheat (Fisher et al. 1992) established that protein transport through the companion cell-sieve tube complex plasmodesmata can occur in both directions, in that <sup>35</sup>S-labeled proteins were detected in the companion cells downstream of the site of phloem loading. At present there is little information available as to the mechanism by which proteins within the translocation stream are transported into the companion cells. The presence, within the phloem sap, of ubiquitin, chaperones (Schobert et al. 1995) and protein kinases (Nakamura et al. 1993, 1996) indicates that protein phosphorylation and chaperones may be involved in this process. In this regard, it is worth noting that a kinase associated with tobacco mesophyll secondary plasmodesmata can phosphorylate the TMV-MP (Citovsky et al. 1993). However, the effect of this phosphorylation on the capacity of the TMV-MP to mediate its cell-to-cell transport has yet to be determined.

It was fortuitous that RPP13-1 was a member of the TRX gene family, as the three-dimensional structure of this protein has been well characterized (Holmgren, 1985). The three-dimensional structures of *E. coli*, *Chlamydomonas* and human TRXs have been determined using X-ray diffraction and nuclear-magnetic-resonance techniques (Katti et al. 1990; Jeng et al. 1994; Qin et al. 1994; Stein et al. 1995; Weichsel et al. 1996; Mittard et al. 1997). Our structure-prediction studies indicated that, as expected, RPP13-1 appears to contain all of the structural elements identified in the bacterial, algal and human TRXs (Fig. 5). Thus, RPP13-1 appears to be a model protein for exploring the structural motifs required for plasmodesmal transport. The sequence comparisons presented in Fig. 4 indicate the close evolutionary relationship between RPP13-1 and TRX genes cloned from *Arabidopsis*, tobacco and *Chlamydomonas* (Brugidou et al. 1993; Rivera-Madrid et al. 1995; Stein et al. 1995). The cytoplasmic TRX of *Chlamydomonas* would not be expected to possess the structural motifs required for cell-to-cell trafficking, as this alga is unicellular in form. On this same note, the f and m forms of the pea chloroplast TRX (Lepiniec et al. 1992; López-Jaramillo et al. 1994), containing the expected N-terminal transit-peptide sequences for import into this organelle, display a similar level of sequence divergence in the MT1 and MT8 regions of the protein.

It is interesting to note that the five N-terminal residues shown to be important in RPP13-1 cell-to-cell transport are absent from the cytoplasmic TRX of *Chlamydomonas*. Furthermore, there is also sequence divergence in the essential MT8 region of RPP13-1 and the *Chlamydomonas* TRX. Interestingly, these residues are conserved in the *Arabidopsis* and tobacco TRX sequences, indicating that these plant proteins may also have the capacity to traffic from cell to cell through plasmodesmata. Future microinjection experiments with these proteins will be performed to test this prediction.

In addition, molecular manipulation of the *Chlamydomonas* TRX, in combination with microinjection experiments will provide a direct test for the involvement of the MT1 and MT8 regions of RPP13-1 in mediating protein trafficking through plasmodesmata. Ultimately, it should be possible to transfer the required plasmodesmal trafficking motifs to the chloroplastic forms of TRX to redirect them for cell-to-cell trafficking rather than import into the chloroplast. (Presumably this would require the removal of the N-terminal TRX m/f transit peptide sequences.)

Studies on TRXs in animals and bacteria indicate that these proteins normally act as general disulfide reductases (Holmgren 1985) and they can regenerate proteins that have been inactivated by oxidative stress in vivo (Fernando et al. 1992) or in vitro (Pigiet and Schuster 1986). The phloem TRX of rice may carry out similar, essential, functions within the sieve tube. In addition, these sieve-tube disulfide reductases may also be involved in regulating ion channel and transporter (sucrose and amino acid) activity across the sieve-tube plasma membrane. Finally, as RPP13-1 moves with the rice phloem translocation stream, we should not overlook the possibility that it, and any of the other 100 or more phloem proteins, may function as a long-distance signaling molecule.

This research was supported in part by a grant from the Human Frontier Science Program (to T.F. and W.J.L.), a Department of Energy Biosciences Grant (DE-FG03-94-ER-06974 to W.J.L.), and a Grant-in-Aid for Scientific Research in Priority Areas (No. 09274101 and No. 09274102 to H.H.). Y.I. was the recipient of an Ezoe-Ikueikai scholarship and a Grant-in-Aid for promotion of Science for Japanese Junior Scientists from the Ministry of Education, Science, Sports and Culture of Japan. Both institutions contributed equally to this study. We also thank H.-L. Wang (UC-Davis) for assistance with the photography. This work is dedicated to Professor Rainer Kollmann on the occasion of his retirement from the Christian-Albrechts-Universität, Kiel, Germany.

## References

- Altschul SF, Gish W, Miller W, Myers EW, Lipman DJ (1990) Basic local alignment search tool. *J Mol Biol* 215: 403–410
- Bostwick DE, Dannenhoffer JM, Skaggs MI, Lister RM, Larkins BA, Thompson GA (1992) Pumpkin phloem lectin genes are specifically expressed in companion cells. *Plant Cell* 4: 1539–1548
- Bower MS, Matias DD, Fernandes-Carvalho E, Mazzurco M, Gu T, Rothstein S, Goring DR (1996) Two members of the thioredoxin-h family interact with the kinase domain of a *Brassica* S locus receptor kinase. *Plant Cell* 8: 1641–1650
- Brugidou C, Marty I, Chartier Y, Meyer Y (1993) The *Nicotiana tabacum* genome encodes two cytoplasmic thioredoxin genes which are differentially expressed. *Mol Gen Genet* 238: 285–293
- Citovsky V, McLean BG, Zupan JR, Zambryski P (1993) Phosphorylation of tobacco mosaic virus cell-to-cell movement protein by a developmentally regulated plant cell wall-associated protein kinase. *Genes Dev* 7: 904–910
- Ding B, Haudenshield JS, Hull RJ, Wolf S, Beachy RN, Lucas WJ (1992) Secondary plasmodesmata are specific sites of localization of the tobacco mosaic virus movement protein in transgenic tobacco plants. *Plant Cell* 4: 915–928
- Eschrich W, Heyser W (1975) Biochemistry of phloem constituents. In: Zimmermann MH, Milburn JA (ed) Encyclopedia of plant physiology, vol 1, Phloem transport. Springer, Berlin, pp 101–136
- Fernando MR, Nanri H, Yoshitake S, Nagata-Kuno K, Minakami S (1992) Thioredoxin regenerates proteins inactivated by oxidative stress in endothelial cells. *Eur J Biochem* 209: 917–922
- Fisher DB, Wu Y, Ku MSB (1992) Turnover of soluble proteins in the wheat sieve tube. *Plant Physiol* 100: 1433–1441
- Gan ZR (1991) Yeast thioredoxin genes. *J Biol Chem* 266: 1692–1696
- Gilbertson RL, Lucas WJ (1996) How do viruses traffic on the 'vascular highway'? *Trends Plant Sci* 1: 260–267
- Hoagland DR, Arnold DI (1938) The water-culture method for growing plants without soil. *Calif Exp Stn Circ* 357: 1–39
- Holmgren A (1985) Thioredoxin. *Annu Rev Biochem* 54: 237–271
- Ishiwatari Y, Honda C, Kawashima I, Nakamura S, Hirano H, Mori S, Fujiwara T, Hayashi H, Chino M (1995) Thioredoxin h is one of the major proteins in rice phloem sap. *Planta* 195: 456–463
- Jeng MF, Campbell AP, Begley T, Holmgren A, Case DA, Wright PE, Dyson HJ (1994) High-resolution structures of oxidized and reduced *Escherichia coli* thioredoxin. *Structure* 2: 853–868
- Johnson TC, Cao RQ, Kung JE, Buchanan BB (1987) Thioredoxin and NADP-thioredoxin reductase from cultured carrot cells. *Planta* 171: 321–331
- Katti SK, LeMaster DM, Eklund H (1990) Crystal structure of thioredoxin from *E. coli* at 1.68 Å resolution. *J Mol Biol* 212: 167–184
- Kawabe S, Fukumori T, Chino M (1980) Collection of rice phloem sap from stylets of homopterous insects severed by YAG laser. *Plant Cell Physiol* 21: 1319–1327
- Kempers R, van Amerongen JK, Achterberg J, van Bel AJE (1996) Exclusion limit of plasmodesmata between sieve element and companion cell in stem of *Vicia faba* is at least 10 kDa. *J Exp Bot* 47: 1298
- Komor E, Orlich G, Weig A, Koßckenberger W (1996) Phloem loading – not metaphysical, only complex: towards a unified model of phloem loading. *J Exp Bot* 47: 1155–1164
- Kouchi H, Hata S (1993) Isolation and characterization of novel nodulin cDNAs representing genes expressed at early stages of soybean nodule development. *Mol Gen Genet* 238: 106–119
- Kühn C, Franceschi VR, Schulz A, Lemoine R, Frommer WB (1997) Macromolecular trafficking indicated by localization and turnover of sucrose transporters in enucleate sieve elements. *Science* 275: 1298–1300
- Lepiniec L, Hodges M, Gadal P, Crépin C (1992) Isolation, characterization and nucleotide sequence of a full-length pea cDNA encoding thioredoxin-f. *Plant Mol Biol* 18: 1023–1025
- López-Jaramillo J, Chueca A, Sahrawy M, Hermoso R, Lázaro JJ, Prado FE, López Gorgé (1994) Cloning and sequencing of a pea cDNA fragment coding for thioredoxin m. *Plant Physiol* 105: 1021–1022
- Lucas WJ, Gilbertson RL (1994) Plasmodesmata in relation to viral movement within leaf tissues. *Annu Rev Phytopathol* 32: 387–411
- Lucas WJ, Ding B, van der Schoot C (1993) Plasmodesmata and the supracellular nature of plants. *New Phytol* 125: 435–476
- Lucas WJ, Bouché-Pillon S, Jackson DP, Nguyen L, Baker L, Ding B, Hake S (1995) Selective trafficking of KNOTTED1 homeo-domain protein and its mRNA through plasmodesmata. *Science* 270: 1980–1983
- Marty I, Meyer Y (1991) Nucleotide sequence of a cDNA encoding a tobacco thioredoxin. *Plant Mol Biol* 17: 143–147
- Mezitt LA, Lucas WJ (1996) Plasmodesmal cell-to-cell transport of proteins and nucleic acids. *Plant Mol Biol* 32: 251–273
- Mittard V, Blackledge MJ, Stein M, Jacquot JP, Marion D, Lancelin JM (1997) NMR solution structure of an oxidised thioredoxin h from the eukaryotic green alga *Chlamydomonas reinhardtii*. *Eur J Biochem* 243: 374–383

- Nakamura S, Hayashi H, Mori S, Chino M (1993) Protein phosphorylation in the sieve tubes of rice plants. *Plant Cell Physiol* 34: 927–933
- Nakamura S, Hayashi H, Mori S, Chino M (1996) Detection and characterization of protein kinases in rice phloem sap. *Plant Cell Physiol* 36: 17–27
- Noueiry AO, Lucas WJ, Gilbertson RL (1994) Two proteins of a plant DNA virus coordinate nuclear and plasmodesmal transport. *Cell* 76: 925–932
- Nguyen L, Lucas WJ, Ding B, Zaitlin M (1996) Viral RNA trafficking is inhibited in replicase-mediated resistant transgenic plants. *Proc Natl Acad Sci USA* 93: 12643–12647
- Peitsch MC (1996) ProMod and Swiss-model: internet-based tools for automated comparative protein modelling. *Biochem Soc Trans* 24: 274–279
- Pigiet VP, Schuster BJ (1986) TRX-catalyzed refolding of disulfide-containing proteins. *Proc Natl Acad Sci USA* 83: 7643–7647
- Qin J, Clore GM, Gronenborn AM (1994) The high-resolution three-dimensional solution structures of the oxidized and reduced states of human thioredoxin. *Structure* 2: 503–522
- Raven JA (1991) Long-term functioning of enucleate sieve elements: possible mechanisms of damage avoidance and damage repair. *Plant Cell Environ* 14: 139–146
- Rivera-Madrid R, Mestres D, Marinho P, Jacquot JP, Decottignies P, Miginiac-Maslow M, Meyer Y (1995) Evidence for five divergent thioredoxin h sequences in *Arabidopsis thaliana*. *Proc Natl Acad Sci USA* 92: 5620–5624
- Sakuth T, Schobert C, Pecsvaradi A, Eichholz A, Komor E, Orlich G (1993) Specific proteins in the sieve-tube exudates of *Ricinus communis* L. seedlings: separation, characterization and in-vivo labeling. *Planta* 191: 207–213
- Schobert C, Großmann P, Gottschalk M, Komor E, Pecsvaradi A, Nieden UZ. (1995) Sieve-tube exudate from *Ricinus communis* L. seedlings contains ubiquitin and chaperones. *Planta* 196: 205–210
- Stein M, Jacquot JP, Jeannette E, Decottignies P, Hodges M, Lancelin JM, Mittard V, Schmitter JM, Miginiac-Maslow M (1995) *Chlamydomonas reinhardtii* thioredoxins: structure of the genes coding for the chloroplastic m and cytosolic h isoforms; expression in *Escherichia coli* of the recombinant proteins, purification and biochemical properties. *Plant Mol Biol* 28: 487–503
- Weichsel A, Gasdaska JR, Powis G, Montfort WR (1996) Crystal structure of reduced, oxidized, and mutated human thioredoxins: evidence for a regulatory homodimer. *Structure* 4: 735–751